UDK 67.017:502.17:669.015.8:669.884:66.040
Original scientific article/Izvirni znanstveni članek

ISSN 1580-2949
MTAEC9, 55(2)171(2021)

DURABILITY PROPERTIES OF RECYCLED CONCRETE WITH LITHIUM SLAG UNDER FREEZE-THAW CYCLES

TRAJNOST RECIKLIRANEGA BETONA Z LITIJEVO ŽLINDRO POD OHLAJEVALNO-SEGREVALNIMI CIKLI

Yongjun Qin*, Jiejing Chen, Ke Liu, Yi Lu

College of Architectural Engineering, Xinjiang University,1230 Yanan Road, Urumqi 830000, China

Prejem rokopisa – received: 2020-07-07; sprejem za objavo – accepted for publication: 2021-12-29

doi:10.17222/mit.2020.126

A water freeze-thaw cycle and sulfate freeze-thaw coupling cycle were explored experimentally to evaluate the durability of recycled concrete with lithium slag (LS). The damage-deterioration law was studied from the aspects of mass-change rate, relative dynamic modulus of elasticity, and cube's compressive strength. Based on the relative dynamic modulus of elasticity, the damage-degree equation of the concrete was fitted, and a mechanical-attenuation model related to this parameter and the cube's compressive strength was established and verified. The damage mechanism under the action of the sulfate freeze-thaw cycle was revealed through scanning electron microscopy (SEM). The combination of recycled coarse aggregate (RCA) and LS was beneficial to the anti-deterioration ability of the concrete. During the cycle experiments, the mass and relative dynamic modulus of elasticity increased initially and then decreased, while the cube's compressive strength declined continually. The concrete with a 30 % RCA substitution rate and 20 % LS exhibited the optimal comprehensive durability, and specimens with excessive LS showed more susceptibility to sulfate erosion. The residual compressive strength of concrete structures can be evaluated by measuring the relative dynamic modulus of elasticity as the two parameters are ideally correlated.

Keywords: recycled concrete, lithium slag, freeze-thaw, attenuation model, SEM

Avtorji so v preizkusu ugotavljali trajnost recikliranega betona z izbrano vsebnostjo litijeve žlindre med procesom združenega ohlajevalno-ogrevalnega (angl.: freeze-thaw cycle) in sulfatno ohlajevalno-ogrevalnega cikla. Zakone slabenja in poškodbe betona so študirali s stališča hitrosti spreminjanja mase, relativnega dinamičnega modula elastičnosti in kubične tlačne trdnosti. Na osnovi relativnega dinamičnega modula elastičnosti so prilagodili enačbo za posamezne stopnje poškodb betona. Postavili in verificirali so model mehanskega slabenja betona v povezavi s tem parametrom in kubično mehansko trdnostjo. Mehanske poškodbe pod vplivom sulfatnega ohlajevalno-ogrevalnega cikla so opazovali z vrstičnim elektronskim mikroskopom (SEM). Ugotovili so, da ima kombinacija grobega recikliranega agregata (RCA) in litijeve žlindre (LS), pozitivni učinek na zmanjšanje slabenja betona. Med eksperimentalnimi cikli sta masa in relativni dinamični modul elastičnosti najprej naraščala in nato začela padati, medtem ko je kubična tlačna trdnost zvezno padala. Beton s 30 % RCA in 20 % LS je imel optimalno trajnost. Preizkušanci s prebitkom LS pa so bili bolj občutljivi na sulfatno erozijo. Avtorji ugotavljajo, da se preostala tlačna trdnost betonskih struktur lahko oceni z merjenjem relativnega dinamičnega modula elastičnosti in da se oba parametra idealno medsebojno ujemata.

Ključne besede: reciklirani beton, litijeva žlindra, ohlajevalno-segrevalni cikel, vrstični elektronski mikroskop, model slabenja

1 INTRODUCTION

Extensive use of concrete materials in the world of architecture necessitates the evaluation of their durability and service life. The damages inflicted to concrete structures as a result of environmental conditions are associated with a variety of complex physiochemical processes. Engineering often encounters freeze-thaw cycles, carbonation, chloride erosion, sulfate erosion or multiple damages caused by two types of synergistic damage reactions, of which the mechanism of action is not a simple superposition.[1,2] Buildings in severely cold areas are often damaged by the freeze-thaw cycle, which is generally considered to be caused by the pressure due to water-freezing expansion of concrete pores as well as seepage pressure.[3] So far, scholars have conducted numerous researches on the freeze-thaw resistance of various concretes and established relevant freeze-thaw damage models.[4–7] In addition to the cold environment, local soils contain abundant sulfate in many parts of the world (e.g., northwest China, the Alps) where concrete engineering is vulnerable to the damage of the coupled freeze-thaw and sulfate corrosion. The coupled degradation mechanism of sulfate and freeze-thaw cycle is complex. On the one hand, the freezing of free water during the freeze-thaw cycle can prevent the entry and reaction of sulfate ions with cement hydration products that form ettringite and gypsum, leading to a disintegration of a gelatinized material. On the other hand, the microcracks formed by the freeze-thaw cycle provide channels for the salt-solution entry as well as further corrosion of the concrete interior, aggravating the concrete deterioration with the repetition effect.[8]

Based on the concept of 'double waste recycling', recycled concrete with lithium slag (LS) is a new type of environmentally friendly building materials with broad application prospects. Its macroscopic mechanical properties have been developed extensively over the years.

*Corresponding author's e-mail:
13144180978@163.com (Yongjun Qin)

Table 1: The chemical composition of cement and LS /%

Materials	CaO	SiO_2	Al_2O_3	Fe_2O_3	SO_3	MgO	Loss	R_2O	K_2O	Na_2O
Cement	55.3	25.4	7.1	2.9	2.8	2.3	2.2	0.9	0.7	0.5
LS	22.0	41.7	18.1	1.2	15.1	0.5	0.4	-	0.3	0.1

Note: LS represents lithium slag

Table 2: Properties of coarse aggregate

Type	Bulk density /kg/m³	Apparent density/ kg/m³	Water absorption /%	Crush value /%	Mud content /%	Fine powder content /%
NCA	1536	2687	0.52	-	0.2	0.2
RCA	1472	2417	3.46	14	0.4	0.5

Note: NCA represents natural coarse aggregate; RCA represents recycled coarse aggregate

LS, the waste from the large-scale production of lithium salt, is a mineral admixture with a composition similar to fly ash and silica fume. Studies confirmed the pozzolanic activity of LS and its micro-aggregate effect after a treatment under certain conditions.[9] With its large production and low costs, LS is considered ideal for recycled concrete. Moreover, experiments proved that recycled concrete with an appropriate amount of LS exhibits better physiomechanical properties than ordinary concrete.[10] Generally, the difference between recycled aggregate and natural aggregate is a distinction in durability between recycled concrete and ordinary concrete, and relevant research has been carried out continuously in the field. V. Bulatović et al.[11] found that the appropriate type of cement could help recycled concrete to exhibit the favorable resistance to sulfate attacks. B. Lei et al.[12] conducted a coupling experiment on recycled concrete during mechanical loading and a freeze-thaw cycle in a salt solution to analyze the influence of a complex environment on its durability. Mineral admixtures were suggested to be used for the improvement of the durability of concrete under certain conditions. Wang et al. experimentally found that an addition of 25 % of fly ash and 5–8 % of silica fume can significantly improve the resistance of recycled concrete to the freeze-thaw and sulfate attack in a 5 % sodium sulfate solution.[13] W. Tian and F. Gao[14] found that under the coupling action of the freeze-thaw cycle and sodium sulfate solution, the concrete with 10 % of fly ash outperformed ordinary concrete in terms of the freeze-thaw resistance in a 5 % sodium sulfate solution.[14]

A thorough investigation of the durability of recycled concrete with LS is of a practical significance, promoting its engineering application. In this research, through an indoor accelerated freeze-thaw method, the freeze-thaw cycle and the coupling effect of freeze-thaw and sulfate were tested on recycled concrete with LS. The effects of the cycle time, RCA substitution rate and LS amount on the mass-change rate, relative dynamic modulus of elasticity (RDME) and cube's compressive strength of the concrete were studied, and a mechanical attenuation model related to the RDME and cube's compressive strength was established. The damage mechanism was further studied using scanning electron microscopy (SEM). This research provides a design basis for the future engineering construction and life prediction.

2 MATERIALS AND EXPERIMENTAL PROCEDURES

2.1 Materials

Ordinary Portland cement of grade 42.5 was used in this experiment. The LS from the Urumqi lithium-salt plant was put into use after being dried and ground. The density and specific surface area of LS were 2.48 g/cm^3 and 417 m^2/kg, respectively. **Table 1** shows the chemical composition of cement and LS.

Fine aggregate is natural medium-coarse sand with a fineness modulus of 3.5, and a polycarboxylic superplasticizer with a 25 % water-reducing rate was adopted in the experiment. RCA came from the demolition site of abandoned buildings in Urumqi. After having been secondarily crushed by a jaw crusher, the particle size was screened and adjusted to a 5–20 mm continuous gradation. The physical-performance indexes of natural coarse aggregate (NCA) and RCA are illustrated in **Table 2**.

2.2 Specimen preparation

A total of 672 specimens were prepared for this experiment. The water-cement ratio of the specimens was 0.45 and the design strength of C30 was selected. The mix proportions of the specimens are listed in **Table 3** with reference to the Chinese standard DG / TJ 08-2018-2007 and the researches by R. Liang and Li.[15–17] The calculation of additional water was based on the water-absorption rate of RCA used in the experiment.

A total of 96 prismoid specimens with dimensions of (100×100×400) mm were used to measure the mass and transverse fundamental frequency alongside 576 cube specimens with dimensions of 100×100×100 mm used to measure the cube's compressive strength. The number of the specimens used for the experiment meets the requirements in accordance with the Chinese standard GB/T50081-2002.[18] Cement, LS, natural sand and natural pebbles were poured sequentially into a HJW60 sin-

Table 3: Design of mix proportions

Code	RCA /%	LS /%	Mix proportion /kg m^{-3}						
			Water	Additional water	Cement	LS	NCA	RCA	Sand
R0L0	0	0	195.00	0.00	433.00	0.00	1221.40	0.00	523.50
R0L20	0	20	195.00	0.00	346.40	86.60	1221.40	0.00	523.50
R30L0	30	0	195.00	7.84	433.00	0	854.98	366.42	523.50
R30L15	30	15	195.00	7.84	368.05	64.95	854.98	366.42	523.50
R30L20	30	20	195.00	7.84	346.40	86.60	854.98	366.42	523.50
R30L25	30	25	195.00	7.84	324.75	108.25	854.98	366.42	523.50
R50L20	50	20	195.00	13.07	346.40	86.60	610.70	610.70	523.50
R70L20	70	20	195.00	18.30	346.40	86.60	366.42	854.98	523.50

Note: R0L0 represents natural concrete; R represents recycled coarse aggregate; L represents lithium slag

gle-shaft mixer to mix them evenly. Afterwards, the previously wetted RCA and water were added to the mixer, and the materials were mixed for 3 min. The formwork was removed after 24 h when the concrete specimens were shaped, and the standard curing was carried out.

2.3 Experimental equipment

A concrete fast freeze-thaw experiment machine and DT-W18 dynamic elastic modulus meter from Beijing Digital zhiyilong Instrument Co., Ltd., were employed in this experiment. The principle of the dynamic elastic modulus meter is to induce a mechanical vibration of the specimens. If the external-force frequency is equal to the fundamental frequency of the specimen, resonance is generated and the amplitude reaches its corresponding maximum. In this way, the dynamic elastic modulus could be calculated using the fundamental frequency. The mass of a specimen was measured with a Hengxin ACS series electronic weighing scale; the cube's compressive strength was gathered by a WAW-1000 electric-hydraulic servo universal test machine.

2.4 Experimental procedure

Half of the specimens from each mix were immersed in a 5-% Na_2SO_4 solution and the other half in water for 4 days after the 24-day standard curing. The liquids had to be kept 20 mm above the surface of the specimens. A complete freeze-thaw cycle lasted for about 4 h. According to the relevant provisions from the Chinese standard GB/T 50082-2009, the average melting time in a freeze-thaw cycle was about 1 hour and 20 minutes and the central temperature in the conditioning chamber was between 7 °C and 19 °C.[19] The specimens were taken out every 25 cycles in order to dry their surfaces and collect the data about the cube's compressive strength, mass change, RDME and obtain SEM pictures. The failure of the concrete specimens was identified when the RDME decreased to 60 % or the mass-change rate reached 5 %.

2.5 Data collection

In this research, three damage indexes were used: the mass change rate, RDME and cube's compressive strength used to analyze the durability of recycled concrete with LS. These indexes can describe the process, from its compactness to looseness, within the concrete structure, representing the overall damage of the specimens to some extent.[20] The mass-change rate is calculated as Equation (1):

$$\Delta W_{Ni} = \frac{W_{0i} - W_{Ni}}{W_{0i}} \cdot 100\ \% \tag{1}$$

Where ΔW_{Ni} is the mass-change rate (%) of a specimen after n cycles; W_{0i} (g) is the initial mass; and W_{Ni} (g) is the mass of a specimen after N cycles.

The RDME is calculated as follows:

$$E_{\mathrm{d}} = 13{,}244 \times 10^{-4} \times \frac{WL^3 F^2}{a^4} \tag{2}$$

$$p_i = \frac{E_{\mathrm{d}N}}{E_{\mathrm{d}0}} \cdot 100\ \% \tag{3}$$

where E_{d} (MPa) is the RDME of a specimen; a(mm) is the side length of a square section; L (mm) represents the length; W (kg) is the mass of a specimen; f (Hz) is the fundamental frequency of a specimen in transverse vibration; p_i represents the RDME reading; $E_{\mathrm{d}N}$ (MPa) represents the dynamic modulus of elasticity after N cycles; and $E_{\mathrm{d}0}$ (MPa) stands for the initial dynamic elastic modulus of a specimen. The cube's compressive strength of specimens was examined under a loading rate of 0.5 MPa/s, and the average value of each group was taken as the final result.

3 RESULTS AND DISCUSSION

3.1 Mass-change rate

The mass-change rate of the specimens increased gradually as the number of freeze-thaw cycles rose. The constant tensile and compressive stress inside the concrete occurred due to the freezing and expansion of free water that resulted in a fatigue failure and specimen mass

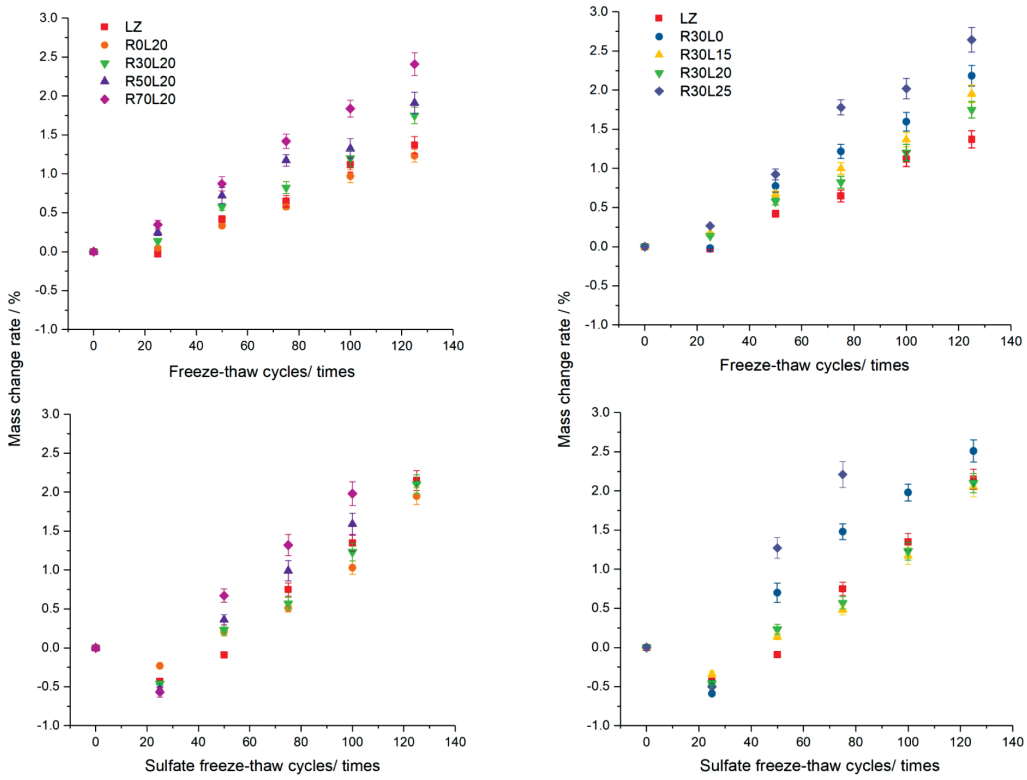

Figure 1: Mass-change rate and cycle experiment: a) R0L0 and specimens with 20 % L, b) R0L0 and specimens with 30 % RCA

changes. Unlike the water freeze-thaw cycle (which is an erosion-failure behavior), the curves for the sulfate freeze-thaw cycle (a complex coupling of surface scaling and internal damage) show an obvious mass increase before the 25th cycle, suggesting that these two cycles have different mechanisms. In the sulfate freeze-thaw cycle, Na_2SO_4 reacts with cement hydration products to produce expansive substances, including gypsum ($CaSO_4 \cdot 2H_2O$) and ettringite ($3CaO \cdot Al_2O_3 \cdot CaSO_4 \cdot 32H_2O$).[21–23] In the early stages of the sulfate freeze-thaw cycle, the amount of erosion causes a mass decrease, thus accounting for a negative growth of the mass-change rate. The chemical-reaction formula of the ettringite sulfate erosion is as follows:

$$Na_2SO_4 \cdot 10H_2O + Ca(OH)_2 \rightarrow CaSO_4 \cdot 2H_2O + 2NaOH + 8H_2O$$

$$4CaO \cdot Al_2O_3 \cdot 13H_2O + 3(CaSO_4 \cdot 2H_2O) + 14H_2O \rightarrow 3CaO \cdot Al_2O_3 \cdot 3CaSO_4 \cdot 32H_2O + Ca(OH)_2$$

In the later period of the cycle experiment, the R0L20 group showed good resistance against the mass change, which proved that the addition of LS moderately improved the compactness of concrete, making the concrete cementation system more stable and resistant against the erosion of freeze-thaw. The change rate of mass is far from a simple linear relationship as it includes a combination of relatively stable and rapid changes, as shown in **Figure 1**. This curve trend is basically consistent with the theory of water segregation and stratification proposed by A. R. Collins who suggests that the frost erosion of concrete is progressive among the surface layers.[24] Under a continuous experiment, an ice layer gradually forms on the surface of the concrete in contact with water. When the frost-heaving force caused by the freeze-thaw environment exceeds its ultimate tensile capacity, the ice layer falls off, thereby changing the concrete quality.

With the same LS amount, a higher substitution rate for RCA leads to a greater mass change and a faster deterioration speed. This is because the water saturation of concrete is one of the most important influential factors when it comes to frost resistance. On the one hand, the initial defects of RCA reduce the compactness and impermeability of concrete, causing more voids and providing the condition for the salt solution and water molecules to enter and accumulate in the interior of the concrete. On the other hand, a large number of interface transition areas of new and old sand slurry further weakens the concrete cohesion and the overall expansion resistance. The experimental group including RCA is less resistant to the mass change than the R0L0 group, and the R30L20 group is the closest to the mass change of the R0L0 group, with a difference in the mass-change rate of only 7 % and 9 %, respectively, after 100 water freeze-thaw cycles and 100 sulfate freeze-thaw cycles.

From another perspective, the difference in the mass change between the water freeze-thaw cycle and sulfate freeze-thaw cycle may be due to the periodic change in the temperature, which leads to a decrease in the solubility of 5 % Na_2SO_4, whose solubility in a saturated solu-

tion (100 g water) at 20 °C is 20.5 g, while in a saturated solution at 10 °C, it decreases to 9.5 g so that crystal precipitation occurs and fills in the pores and microcracks. The specific reaction equation is as follows:

$$Ca(OH)_2 + Na_2SO_4 \rightarrow Ca^{2+} + SO_4^{2-} + Na^+ + OH^-$$

$$Ca(OH)_2 + Na_2SO_4 + 2H_2O \rightarrow CaSO_4 \cdot 2H_2O + 2NaOH$$

The mass-change rate of the specimens showed an obvious difference between the sulfate freeze-thaw and water freeze-thaw, especially in the later stage of the cyclic experiment. After 100 cycles, the mass-change rate of almost all the experimental groups exposed to the sulfate freeze-thaw cycles was higher than for those exposed to the water freeze-thaw cycles. Amongst them, R50L20, R70L20 and R30L25 were intensely damaged under the sulfate freeze-thaw experimental conditions so that no effective data could be obtained, indicating a serious deterioration effect of the sulfate corrosion. It is also worth mentioning that after 100 cycles, the mass-change-rate difference for the R0L20 group under water freeze-thaw cycles and sulfate freeze-thaw cycles could be reduced to 6 %, which proves that 20 % of LS could ensure that the specimens exhibited an adequate sulfate resistance to a certain extent.

3.2 Relative dynamic modulus of elasticity (RDME)

3.2.1 Trend analysis

The R30L20 group with the slowest RDME decline rate in the first 25 cycles under the two conditions still maintained the maximum value after 125 cycles, which was 11 % and 12 % higher than that of ordinary concrete, respectively, displaying better durability, as shown in **Figure 2**. The RDME increases with the addition of pozzolanic LS in an amount below 20 %. The secondary hydration reaction between LS and $Ca(OH)_2$, the product of cement hydration, produces large amounts of densely structured C-S-H and C-A-H cementitious materials, which can obviously change the transverse fundamental frequency. Simultaneously, the cementitious materials can effectively fill in the pores of concrete, making up for the RCA-caused decline in the concrete permeability and reducing the damage caused by the early freeze-thaw cycle.[25,26]

The most serious damage occurred in R30L25 with an accompanied slow hydration rate. In the middle and later periods of the sulfate freeze-thaw cycle, the RDME of R50L20 and R70L20 decreases sharply, falling below the levels of R0L0. The RDME degradation rate of the 70-% RCA is evidently faster than that of ordinary concrete. According to the classical critical water saturation theory, concrete is easily damaged when the water saturation of concrete mortar reaches a certain level.[27] RCA with old mortar induces water absorption by microcracks, reaching the critical saturation level, and the interface transition zone between old and new mortars can easily produce the osmotic pressure, aggravating the damage to the concrete. However, after the water freeze-thaw cycle, the RDME of R50L20 is higher than

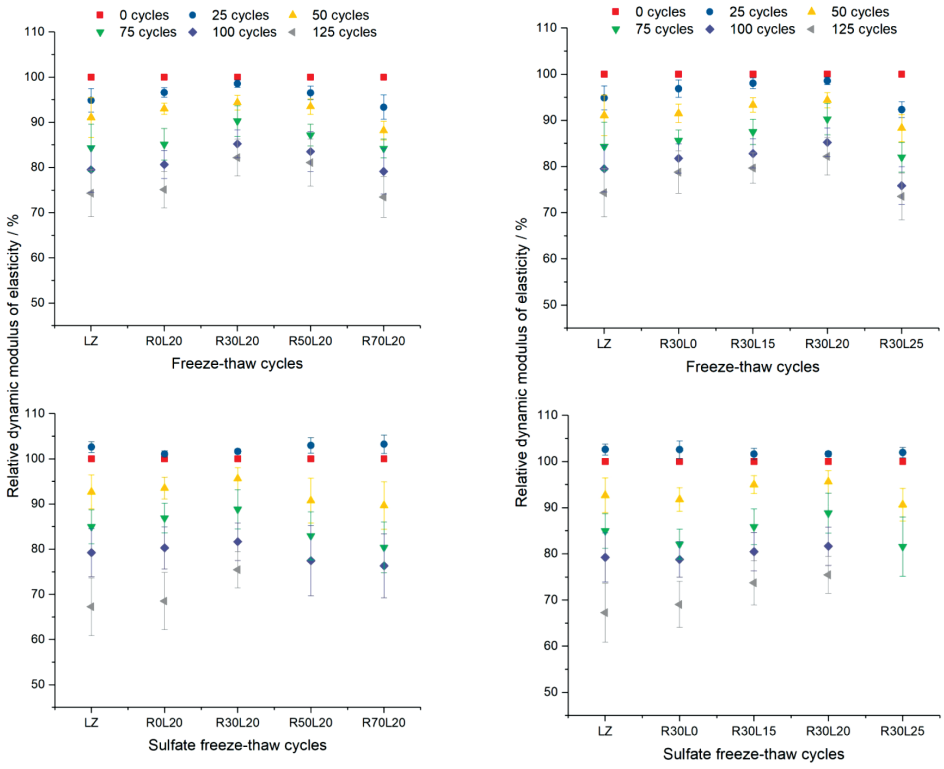

Figure 2: Relative dynamic modulus of elasticity and the cyclic experiment: a) R0L0 and specimens with 20 % LS, b) R0L0 and specimens with 30 % RCA

that of R0L0, which supports the theory proposed by M. Mao et al.,[28] according to which the porous and loose microstructure of RCA can play a role in dispersing the condensation-water pressure to a certain extent. Therefore, during a practical application of the recycled concrete mixed with LS, its proportion issue, in combination with environmental factors, needs to be considered.

According to the basic principle of the damage mechanics of concrete, p_i is the freeze-thaw damage variable.[20] Damage factor D can be defined as:

$$D(N) = \frac{E_N - E_0}{E_0} \cdot 100\ \% \tag{4}$$

where E_N is the dynamic elastic modulus after N cycles of the sulfate freeze-thaw; and E_0 is the initial dynamic elastic modulus. The relative damage degree of a concrete specimen after N freeze-thaw cycles can be defined as G_i:

$$G_i = \frac{D_i(N)}{D_0(N)} \tag{5}$$

where $D_0(N)$ and $D_i(n)$ are the damage factors of the concrete specimen after N cycles of the water freeze-thaw and Na_2SO_4 freeze-thaw, respectively. G_i reveals the difference between the mechanisms of the water freeze-thaw cycle and sulfate freeze-thaw cycle.

Before the 25th cycle, the mechanism of water freeze-thaw is almost opposite to that of sulfate freeze-thaw, as shown in **Figure 3**. After the 50th cycle, as a result of the salt solution having a lower freezing point than water, the actual freezing duration of the specimens is far shorter than that of the liquid water in the same cycle, hence limiting the early sulfuric acid ion erosion effect.[29] Damages made to most of the specimens are quite similar, so the relative damage degrees of most groups are close to 1. As the cycle experiment continues, the relative damage is gradually intensified, indicating that the negative effect of the sulfate erosion is increasingly obvious.[25,30] In the experimental process, the sulfate-enhanced erosion occurred the earliest in the R50L20 group, and the R30L25 group failed the earliest. After 100 cycles, the relative damage degrees of the R30L20 group and R30L0 group were the largest, proving that the positive effect of 20 % of LS on the RDME was gradually offset by the sulfate corrosion. Hence, most of C-S-H and C-A-H were decalcified and decomposed at this time, and the negative effect of sulfate was dominant. The increase in the relative damage degree in the later stage shows that the damage caused by sulfate freeze-thaw is much faster than that caused by water freeze-thaw.

3.2.2 RDME damage model

In accordance with the changing law of the RDME of the recycled concrete with LS under freeze-thaw cycle and the classical freeze-thaw damage model, the following exponential relationship can be established:[31]

$$P_N = \alpha e^{\beta N} \tag{6}$$

where p_i is the RDME of the material (%); N is the number of the freeze-thaw cycles; α is the material coefficient; and β is the attenuation coefficient. The fitted curve and correlation fitting parameters are shown in **Table 4**.

As far as the goodness-of-fit is concerned, the RDME model based on the attenuation coefficient and material coefficient is not as applicable to the sulfate freeze-thaw cycle as to the water freeze-thaw cycle, especially for the group with a high LS amount and high RCA substitution rate. Specifically, the fitting coefficient for R30L25 is only 0.731, and for R70L20, it is only 0.817. In this regard, Zhao proposed a more universal quadratic polynomial function:[32]

$$P_N = A \cdot x^2 + B \cdot x + C \tag{7}$$

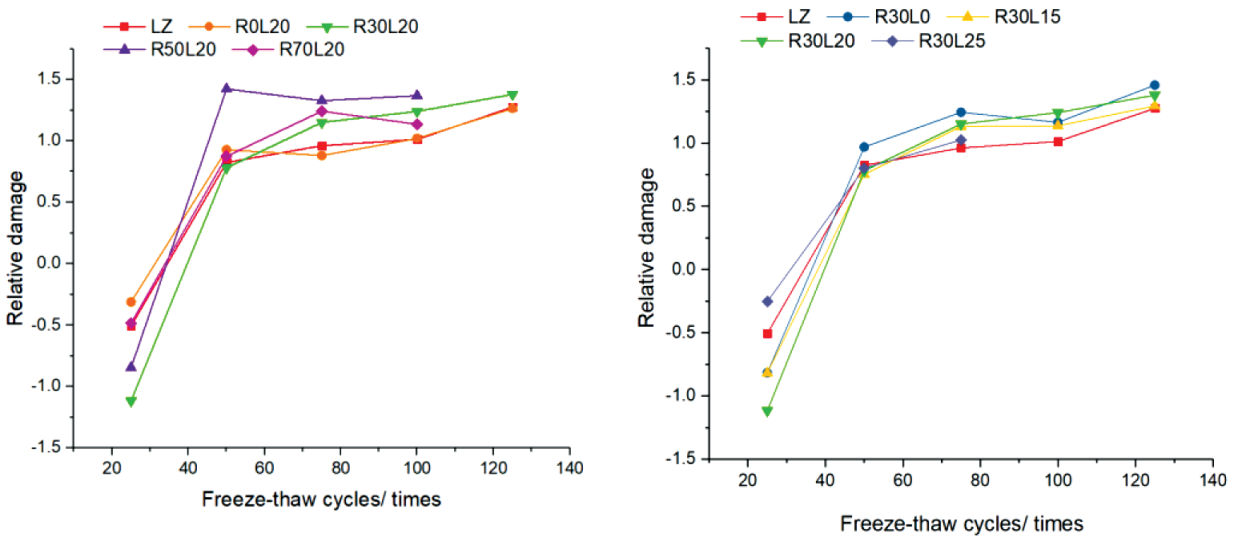

Figure 3: Relative-damage-degree trend: a) R0L0 and specimens with 20 % LS, b) R0L0 and specimens with 30 % RCA

Table 4: Correlation fitting parameters (1)

Group		R0L0	R0L20	R30L0	R30L15	R30L20	R30L25	R50L20	R70L20
α		100.74	101.66	100.70	101.46	101.47	99.40	100.57	99.69
$\beta/10^{-3}$	water	–2.36	–2.31	–2.02	–1.93	–1.65	–2.53	–1.77	–2.37
	sulfate	–2.54	–2.49	–2.58	–2.24	–2.03	–2.07	–2.35	–2.46
R^2	water	0.991	0.978	0.988	0.977	0.978	0.988	0.986	0.996
	sulfate	0.864	0.885	0.888	0.902	0.892	0.731	0.843	0.817

Note: a represents the material coefficient; β represents the attenuation coefficient; R^2 represents the goodness of fit

Table 5: Correlation fitting parameters(2)

Group	R0L0	R0L20	R30L0	R30L15	R30L20	R30L25	R50L20	R70L20
$A/10^{-3}$	–1.60	–1.72	–0.90	–1.05	–1.25	–4.40	–1.42	–1.18
$B/10^{-3}$	–76.09	–43.55	–156.43	–101.49	–60.70	–63.87	–118.19	–163.23
C	101.70	100.96	102.34	101.82	101.46	100.77	102.06	102.49
R^2	0.973	0.988	0.952	0.968	0.978	0.955	0.921	0.902

where A, B are the coefficients; and C is the intercept. The fitting effect is shown in **Table 5**.

The quadratic function outperforms the exponential function in its description of the damage process for the recycled-concrete mixed with LS under a sulfate attack. The average optimization degree of R^2 is 12.32 % with a maximization of 30.59 %, which is more consistent with the reference requirements of practical engineering.

3.3 Cube's compressive strength

The cube's compressive strength reflects the overall failure of specimens.[33] Unlike the ascending curves of the mass-change rate and RDME emerging in a sulfate freeze-thaw cycle, the cube's compressive strength of the specimens decreases throughout the cycle experiment, with a greater decline range in the later cycles, as shown in **Figure 4**. With the increase in the number of cycles, the change of mortar and the intensification of internal cracks led to a reduction in the concrete stress area and horizontal binding force, causing the surface to peel off with more ease from the whole specimen upon compression. Apparently, the specimens were severely denudated after multiple cycles, resulting in the exposed surface to be uneven. After repeated cycles, at the macro-strength

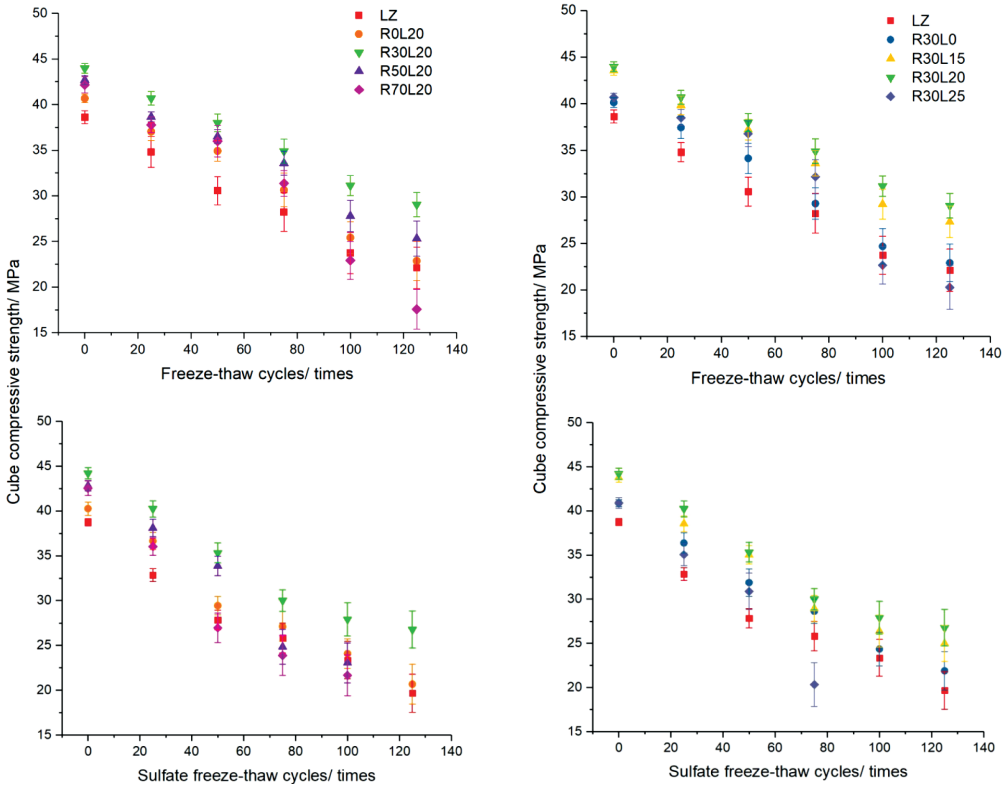

Figure 4: Cube's compressive strength and cyclic experiment: a) R0L0 and specimens with 20 % LS, b) R0L0 and specimens with 30 % RCA

level, the cube's compressive strength of most recycled concrete with LS was evidently higher than that of ordinary concrete.

Generally, the specimens with a larger relative strength have a higher relative-strength surplus after the cycle experiments. The anti-sulfate freeze-thaw strength degradation is optimized with the addition of 30 % of RCA, but excessive RCA will enlarge the spalling-transition area inside the specimens where cracks easily widen and propagate. In terms of the failure form, however, bone destruction rarely occurs in the specimens. The use of LS contributes to the alleviation of the deterioration of compressive strength. Secondary hydration reaction plays a positive role in both water freeze-thaw and sulfate freeze-thaw.[34,35] However, an excessive use of LS, instead of cement, is equivalent to an increase in the effective water-cement ratio, resulting in the alteration of the concrete's internal-water saturation, which is an important influence factor for the freeze-thaw damage. In the middle and later periods of a cycle experiment, the development trend of the cube's compressive strength in each group is similar to that of the RDME.

3.4 Compressive-strength attenuation model

The freeze-thaw damage of concrete is evaluated primarily with two indexes: the RDME and mass-change rate, which mostly require non-destructive tests. Destructive tests are still needed to understand the whole mechanical-degradation law of concrete under the action of freeze-thaw. Results show the RDME to be sensitive to the number of freeze-thaw cycles, ultimately defining the freeze-thaw damage of concrete. The deterioration of the cube's compressive strength with freeze-thaw cycles can be expressed with a function including RDME.

The cube's compressive strength is inversely proportional to the number of freeze-thaw cycles, and the curve can be regarded as a continuous differentiable function.[36] If the cube's compressive strength of a specimen after 0 cycles is f_0 and it is $f(N)$ after N cycles, then the decay rate of the compressive strength after $N + \Delta N$ cycles is as follows:

$$\frac{f(N+\Delta N)-f(N)}{f(N)} = \lambda_1 \Delta N \tag{8}$$

where λ_1 (< 0) is the constant representing the loss of compressive strength per freeze-thaw cycle.

Equation (8) can be transposed as:

$$\frac{\mathrm{d}f(N)}{\mathrm{d}N} = \lambda_1 f(N) \tag{9}$$

After integration:

$$\frac{f(N)}{f_0} = e^{\lambda_1 N} \tag{10}$$

Similarly, the RDME of concrete is inversely proportional to the number of freeze-thaw cycles, hence the relationship between the two functions can be regarded as a differentiable function. By referring to the above freeze-thaw damage-index model (6), the formula can be transposed as:

$$N = \frac{1}{\beta} \ln \frac{P_N}{a} \tag{12}$$

Integrating the relationship between the RDME and cube's compressive strength yields:

$$\frac{f(N)}{f_0} = \frac{1}{a} P_N^{\frac{\lambda_1}{\beta}} \tag{13}$$

Where $1/a = k_1$ and $\lambda_1/\beta = b_i$. The relative residual strength of a concrete specimen is:

$$\frac{f(N)}{f_0} = k_i P_N^{b_1} \tag{14}$$

Clearly, the relationship between the relative residual compressive strength and RDME follows a power function. For a given RDME, the cube's compressive strength and the number of freeze-thaw cycles of the specimens do not strictly obey the inverse proportional function; therefore, k_i and b_i can be determined according to the above model fitting correction based on the experiment results. The specific values are shown in **Table 6**.

As seen from **Table 6**, the fitting coefficient R^2 is more than 0.88 for all groups, exceeding 95 % in 62.5 % of the groups under water freeze-thaw and 50 % of the groups under sulfate freeze-thaw, indicating an ideal correlation between the performance indexes and verifying the rationality and reliability of the model. Therefore, the residual strength of concrete structures in similar environments can be estimated with the RDME.

4 MICROSCOPIC-MECHANISM ANALYSIS

Based on the above damage-index analysis, three most representative groups, R30L25, R30L20 and R70L20, were selected for a microstructure analysis to further explore the damage mechanism after erosion due to the sulfate freeze-thaw cycles. After 25 cycles, fewer

Table 6: Fitting-coefficient value

Group	R0L0	R0L20	R30L0	R30L15	R30L20	R30L25	R50L20	R70L20		
Medium	water	k_i	100.94	100.33	98.52	101.97	102.34	91.73	99.06	93.67
		b_i	0.52	0.50	0.40	0.54	0.53	0.33	0.40	0.28
	$NaSO_4$	k_i	118.64	110.06	110.59	110.91	109.61	105.16	106.41	114.58
		b_i	0.81	0.64	0.73	0.67	0.65	0.38	0.50	0.59

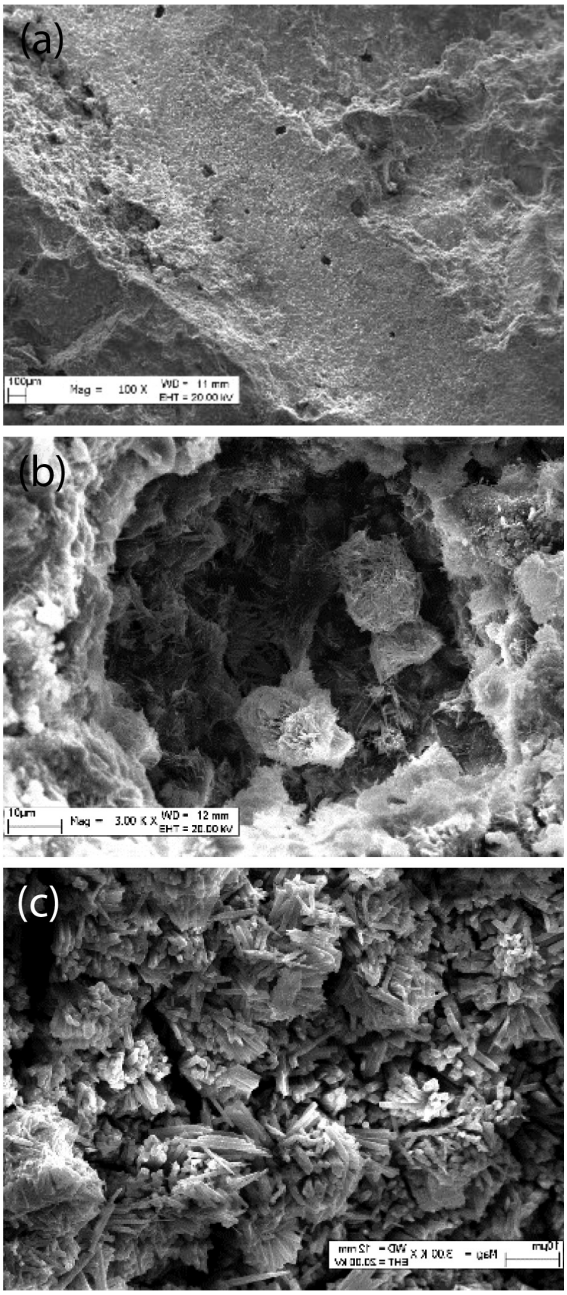

Figure 5: SEM pictures of R30L25: a) after 25 cycles, b) after 75 cycles, c) after 100 cycles

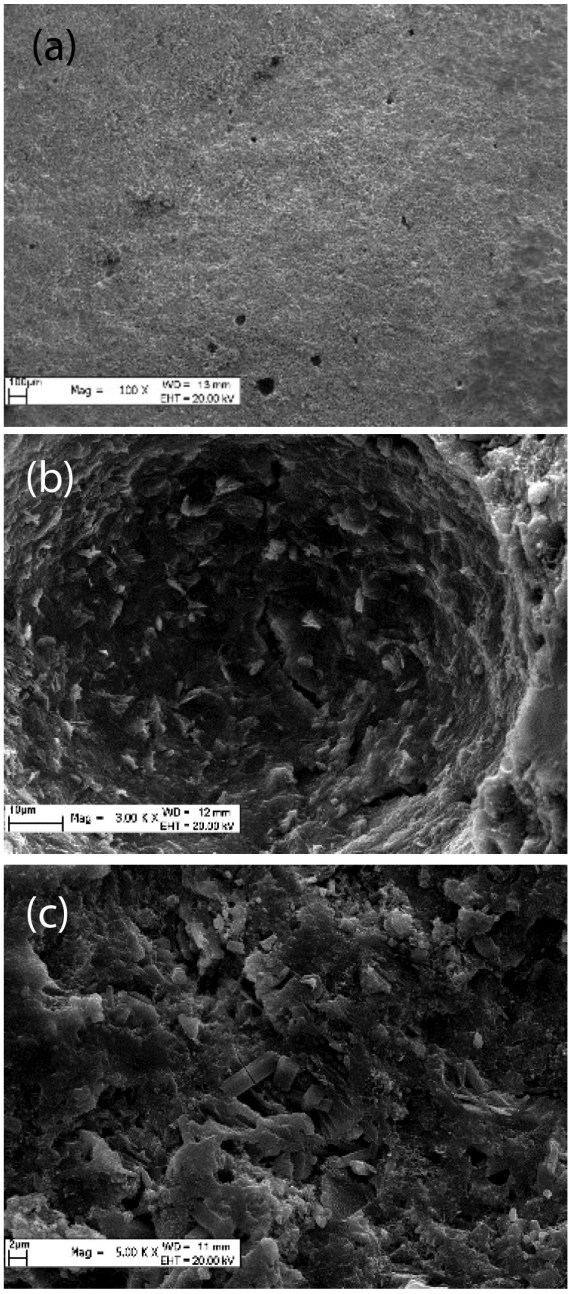

Figure 6: SEM pictures of R30L20: a) after 25 cycles, b) after 75 cycles, c) after 100 cycles

microcracks formed in each group of the concrete specimens, and the interiors showed a uniform continuum, as shown in **Figures 5a** to **7a**. A good spatial network structure was formed between hydration products and aggregates with smooth and regular pore walls, suggesting the necessity of the internal space within the specimens for stress relief due to a volume expansion.

SEM images show the microstructure of R30L25 with incomplete hydration to be relatively loose and not as smooth as the other two groups, facilitating the penetration of sodium sulfate solution and providing an explanation for the largest mass increase of R30L25.[37] After 75 cycles, the microstructures of the three groups were obviously damaged, especially in R30L25 where abundant corrosion products appeared, as seen on **Figures 5b** to **7b**. An energy spectrum analysis showed that the main elements are Al, Si, Ca and O, confirming that the needle-like corrosion crystals are mainly ettringite.[38] Both R30L20 and R70L20 have a loose and flocculent colloidal structure, while microcracks are densely distributed and mutually crossing, indicating the macroscopic performance involving an increased mass-change rate, and decreased RDME and cube's compressive strength.

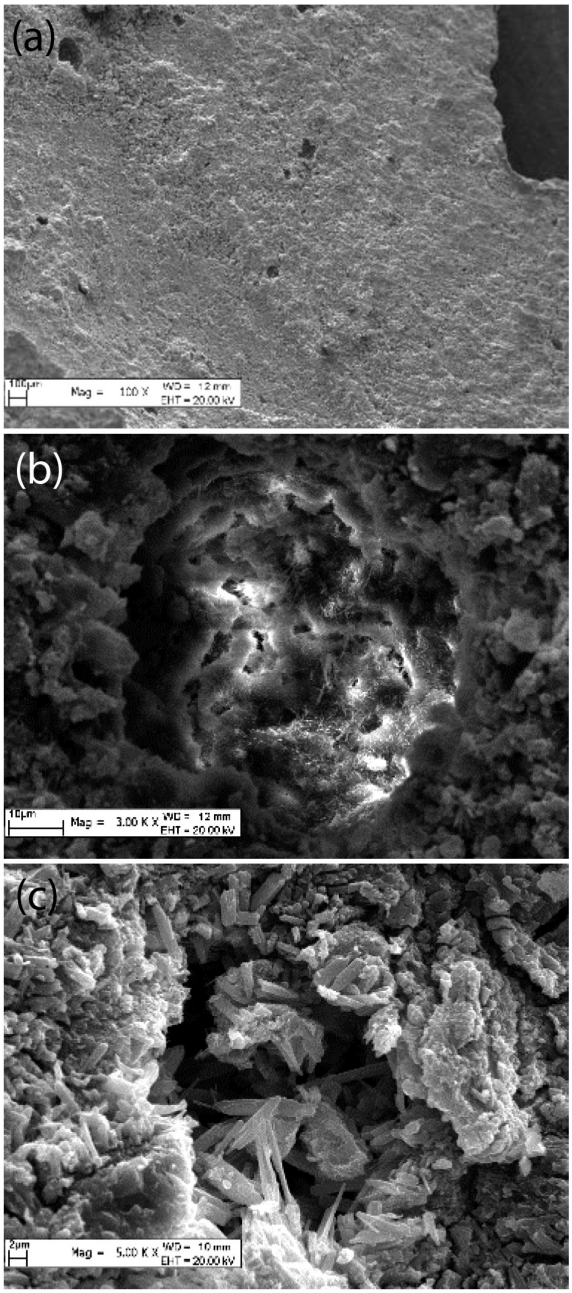

Figure 7: SEM pictures of R70L20: a) after 25 cycles, b) after 75 cycles, c) after 100 cycles

With further sulfate freeze-thaw corrosion, a mass of corrosive products appeared in all three groups. Expansive products (e.g., acicular ettringite and short-column $Ca_2SO_4{\cdot}2H_2O$), gathering in large quantities and occupying the pore space were formed after cement hydration (**Figures 5c** to **7c** extending predominantly beyond the range of the pore interior.[39] Among them, internal corrosive products evidently occupy a large part of the internal structure of R30L25. Based on the three damage indexes, it is easily proven that R30L25 failed first. Further development of internal cracks in the other two groups led to a reduction in the cohesion and compactness of the concrete, leading to a decreased macroscopic performance of the concrete and accelerated inward entrance of the solution. The increase in the SO_4^- concentration indicates augmented quantities of expansible products (e.g., ettringite and flaky gypsum), which accelerated the corrosion and fundamentally destroyed the specimens. The deterioration of the internal structure was more intense in R70L20 than in R30L20, which had a lower macroscopic damage index.

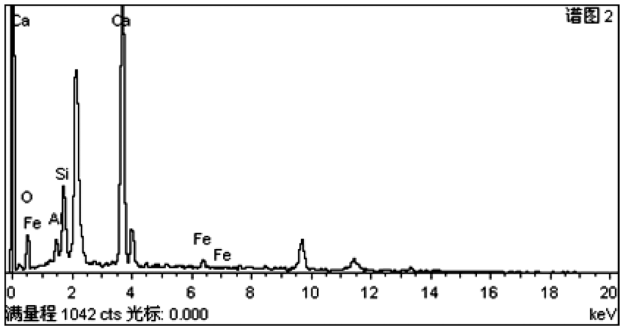

Figure 8: Elemental analysis of R30L25

5 CONCLUSIONS

The survey of recycled concrete with LS investigates different elements of durability under the conditions of water freeze-thaw cycles and sulfate freeze-thaw cycles. In the early stage of cycles, water freeze-thaw and sulfate freeze-thaw have similar effects on the specimens; however, with the increase in the number of cycles, the damage of sulfate freeze-thaw was accelerated, showing a more serious deterioration.

In the sulfate freeze-thaw, the mass-change rate and RDME increase in the early stage, while the cube's compressive strength is unaffected by certain fine cracks and declines. R30L20 displays the optimal durability, whilst R30L25 exhibits an inadequate antifreeze performance.

Additionally, the new mechanical attenuation model, related to the RDME and cube's compressive strength, was verified with respect to its rationality and reliability. This model can be used to evaluate the residual cube's compressive strength of the recycled concrete with LS in cold regions.

The microstructure analysis illustrates the conditions for an incomplete hydration reaction caused by excessive LS and its impact on the acceleration of the internal-structure deterioration of concrete under external conditions.

Acknowledgment

This work was fully supported by a grant from the National Natural Science Foundation of China (Study on the performance and constitutive relation of recycled concrete with lithium slag as a mineral admixture), China (Project No. 51668061).

6 REFERENCES

[1] S. Zhang, B. Zhao, Research on the performance of concrete materials under the condition of freeze-thaw cycles, Eur. J. Environ. Civ. En., 17 (**2013**) 860–871, doi:10.1080/19648189.2013.826601

[2] J. Gong, J. Cao, Y. Wang, Effects of sulfate attack and dry-wet circulation on creep of fly-ash slag concrete, Constr. Build. Mater., 125 (**2016**), 12–20, doi:10.1016/j.conbuildmat.2016.08.023

[3] R. Zhao, Y. Yuan, Z. Cheng, T. Wen, J. Li, F. Li, Z. J. Ma, Freeze-thaw resistance of Class F fly ash-based geopolymer concrete, Constr. Build. Mater., 222 (**2019**) 474–483, doi:10.1016/j.conbuildmat.2019.06.166

[4] P. J. Tikalsky, J. Pospisil, W. MacDonald, A method for assessment of the freeze–thaw resistance of preformed foam cellular concrete, Cement Concrete Res., 34 (**2004**) 889–893, doi:10.1016/j.cemconres.2003.11.005

[5] A. E. Richardson, K. A. Coventry, S. Wilkinson, Freeze/thaw durability of concrete with synthetic fibre additions, Cold Reg. Sci. Technol., 83–84 (**2012**) 49–56, doi:10.1016/j.coldregions.2012.06.006

[6] C. Karakurt, Y. Bayazıt, Freeze-thaw resistance of normal and high strength concretes produced with fly ash and silica fume, Adv. Mater. Sci., Eng., 2015 (**2015**) 1–8, doi:10.1155/2015/830984

[7] Y. Fu, L. Cai, W. Yonggen, Freeze–thaw cycle test and damage mechanics models of alkali-activated slag concrete, Constr. Build. Mater., 25 (**2011**) 3144–3148, doi:10.1016/j.conbuildmat.2010.12.006

[8] H. A. F. Dehwah, Effect of sulfate concentration and associated cation type on concrete deterioration and morphological changes in cement hydrates, Constr. Build. Mater., 21 (**2007**), 29–39, doi:10.1016/j.conbuildmat.2005.07.010

[9] W. Yiren, W. Dongmin, C. Yong, Z. Dapeng, L. Ze, Micro-morphology and phase composition of lithium slag from lithium carbonate production by sulphuric acid process, Constr. Build. Mater., 203 (**2019**) 304–313, doi:10.1016/j.conbuildmat.2019.01.099

[10] Y. Qin, J. Chen, Z. Li, Y. Zhang, The mechanical properties of recycled coarse aggregate concrete with lithium slag, Adv. Mater. Sci. Eng., 2019 (**2019**), 1–12, doi:10.1155/2019/8974625

[11] V. Bulatović, M. Melešev, M. Radeka, V. Radonjanin, I. Lukić, Evaluation of sulfate resistance of concrete with recycled and natural aggregates, Constr. Build. Mater., 152 (**2017**) 614–631, doi:10.1016/j.conbuildmat.2017.06.161

[12] B. Lei, W. Li, Z. Tang, V. W. Y. Tam, Z. Sun, Durability of recycled aggregate concrete under coupling mechanical loading and freeze-thaw cycle in salt-solution, Constr. Build. Mater., 163 (**2018**) 840–849, doi:10.1016/j.conbuildmat.2017.12.194

[13] D. Wang, X. Zhou, Y. Meng, Z. Chen, Durability of concrete containing fly ash and silica fume against combined freezing-thawing and sulfate attack, Constr. Build. Mater., 147 (**2017**),398–406, doi:10.1016/j.conbuildmat.2017.04.172

[14] W. Tian, F. Gao, Damage and degradation of concrete under coupling action of freeze-thaw cycle and sulfate attack, Adv. Mater. Sci. Eng., 2020 (**2020**) 1–17, doi:10.1155/2020/8032849

[15] DG/TJ 08-2018-2007: The technical code on the application of recycled concrete, China, 2007

[16] R. Liang, Study on the performance and application of recycled coarse aggregate of waste concrete in Urumqi, China, Xinjiang University, 2014

[17] L. Li, Design and performance of recycled concrete mix of mineral admixture in the cold region of Xinjiang, China, Xinjiang University, 2014

[18] GB/T 50081-2002: Test method for mechanical properties of ordinary concrete, China, 2003

[19] GB/T 50082-2009: Standard test methods for long-term performance and durability of ordinary concrete, China, 2009

[20] X. Ren, X. M. Wang, T. J. Zhao, Research progress and model review of freezing-thawing and salt-freezing degradation mechanism of concrete, Concrete, 9 (**2012**) 15–18, doi:10.3969/j.issn.1002-3550.2012.09.006

[21] W. Qiu, F. Teng, S. Pan, Damage constitutive model of concrete under repeated load after seawater freeze-thaw cycles, Constr. Build. Mater., 236 (**2020**), 117560, doi:10.1016/j.conbuildmat.2019.117560

[22] W. L. Jia, H. Li, Q. Zhang, Frost resistance of recycled aggregate concrete under sulfate environment, Silicate Bulletin, 35 (**2016**), 1816–1820, doi:10.16552/j.cnki.issn1001-1625.2016.06.031

[23] H. Siad, M. Lachemi, M. Şahmaran, K. M. A. Hossain, Preconditioning method for accelerated testing of concrete under sulfate attack, ACI Mater. J., 113 (**2016**), 222–225, doi:10.14359/51688705

[24] A. R. Collin, The destruction of concrete by frost, Journal of Institution of Civil Engineers, 23 (**1944**), 29–41, doi:10.1680/ijoti.1944.14086

[25] Y. Li, R. Wang, S. Li, Y. Zhao, Y. Qin, Resistance of recycled aggregate concrete containing low- and high-volume fly ash against the combined action of freeze–thaw cycles and sulfate attack, Constr. Build. Mater., 166 (**2018**), 23–34, doi:10.1016/j.conbuildmat.2018.01.084

[26] F. U. A. Shaikh, S. W. M. Supit, Compressive strength and durability properties of high volume fly ash (HVFA) concretes containing ultrafine fly ash (UFFA), Constr. Build. Mater., 82 (**2015**), 192–205, doi:10.1016/j.conbuildmat.2015.02.068

[27] G. Fagerlund, The significance of critical degrees of saturation at freezing of porous and brittle materials, Durability of Concrete: American Concrete Institute, Detroit 1975, 13–65

[28] M. Mao, D. Zhang, Q. Yang, W. Zhang, Study of durability of concrete with fly ash as fine aggregate under alternative interactions of freeze-thaw and carbonation, Adv. Civ. Eng., 2019 (**2019**) 1–15, doi:10.1155/2019/4693893

[29] Q. H. Xiao, Q. Li, Z. Y. Cao, W. Y. Tian, The deterioration law of recycled concrete under the combined effects of freeze-thaw and sulfate attack, Constr. Build. Mater., 200 (**2019**) 344–355, doi:10.1016/j.conbuildmat.2018.12.066

[30] L. Jiang, D. Niu, L. Yuan, Q. Fei, Durability of concrete under sulfate attack exposed to freeze–thaw cycles, Cold Reg. Sci. Technol., 112 (**2015**) 112–117, doi:10.1016/j.coldregions.2014.12.006

[31] J. G. Niu, F. L. Zuo, J. L. Wang, C. B. Xie, Freeze-thaw damage model of plastic-steel fiber reinforced lightweight aggregate concrete, Journal of Building Materials, 21 (**2018**), doi:10.3696/j.issn.1007-9629.2018.02.010

[32] Y. R. Zhao, J. Gao, L. Wang, Z. L. Guo, Study on frost resistance of basalt fiber concrete under unilateral freezing and thawing, Concrete, 4 (**2020**), 70–73, doi:10.3969/j.issn.1002-3550.2020.04.017

[33] M. Sun, D. Xin, C. Zou, Damage evolution and plasticity development of concrete materials subjected to freeze-thaw during the load process, Mech. Mater., 139 (**2019**), 103192, doi:10.1016/j.mechmat.2019.103192

[34] D. Zhang, M. Mao, Q. Yang, W. Zhang, P. Han, Experimental investigation of neutralisation of concrete with fly ash as fine aggregate in freeze-thaw environment, Adv. Civ. Eng., 2019 (**2019**), 1–12, doi:10.1155/2019/6860293

[35] L. J. Malvar, L. R. Lenke, Efficiency of fly ash in mitigating alkali-silica reaction based on chemical composition, ACI Mater. J., 103 (**2016**), 319–326, doi:10.3166/rmpd.7.543-554

[36] C. D. Xu, Z. Li, X. L. Zhu, Z. P. Yao, M. Y. Wang, P. Zhang, Study on mechanical properties of concrete under salt-frost erosion, Yellow River, doi:10.3696/j.issn.1000-1379.2019.09.028

[37] D. Zhang, M. Mao, S. Zhang, Q. Yang, Influence of stress damage and high temperature on the freeze–thaw resistance of concrete with fly ash as fine aggregate, Constr. Build. Mater., 229 (**2019**), 116845, doi:10.1016/j.conbuildmat.2019.116845

[38] H. Nguyen, T. Chang, J. Shih, C. Chen, Influence of low calcium fly ash on compressive strength and hydration product of low energy super sulfated cement paste, Cem. Concr. Comp., 99 (**2019**) 40–48, doi:10.1016/j.cemconcomp.2019.02.019

[39] M. F. Najjar, M. L. Nehdi, A. M. Soliman, T. M. Azabi, Damage mechanisms of two-stage concrete exposed to chemical and physical sulfate attack, Constr. Build. Mater., 137 (**2017**) 141–152, doi:10.1016/j.conbuildmat.2017.01.112